Journal of Materials Chemistry B

Accepted Manuscript

ROYAL SOCIETY OF CHEMISTRY

www.rsc.org/materialsB

This paper examined how examining how the pore curvature perturbed the protein structure, by multiscale approaches including HPLC, confocal, NMR &H/D exchange, molecular docking simulations.

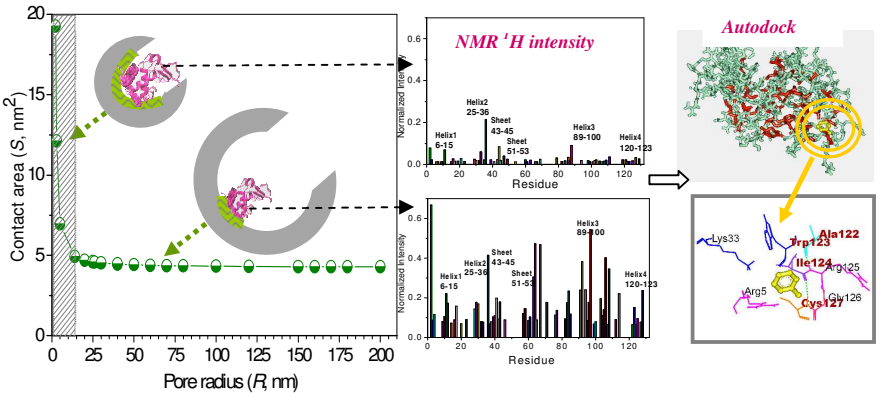

Journal of Materials Chemistry B

Cite this: DOI: 10.1039/c0xx00000x

ARTICLE TYPE

www.rsc.org/xxxxxx

Multiscales evaluation of pore curvature effects on protein structure in nano pores

Dong-Xia Hao,[a] Yong-Dong Huang,[a] Kang Wang,[b] Yuping Wei,[a] Weiqing Zhou,[a] Juan Li,[a] Guang-Hui Ma*[a] and Zhi-Guo Su*[a]

Received (in XXX, XXX) Xth XXXXXXXXX 20XX, Accepted Xth XXXXXXXXX 20XX
DOI: 10.1039/b000000x

Protein structure in nano pore is an important determinant in porous substrates utilization in biotechnology and materials science. To date, accurate residue details of pore curvature induced protein binding and unfolding were still unknown. Here, multiscale ensemble of chromatography, NMR hydrogen and deuterium (H/D) exchange, confocal scanning and molecular docking simulations was combined to obtain the protein adsorption information induced by pore size and curvature. Lysozyme and polystyrene microspheres within pores range in 14-120 nm were respectively utilized as models. With pores size increasing, the bound lysozyme presented a tendency with significant decreased retention, less unfolding and less interacted sites. However, such significant dependence between pore curvature and protein size only existed in a limited micro-pore range comparable to protein. The mechanism behind above events could be attributed to the diverse protein's interaction area tailed by pores curvature and size change, by models calculating the binding of lysozyme onto surfaces. Another surface of opposite curvature for nanoparticle were also calculated and compared, the rules was similar but with opposite direction and such critical size also existed. These studies of protein on curved interface may ultimately help guide the design of novel porous materials and assist to discriminate the target protein from molecular banks.

1 Introduction

Protein interaction with nanoporous substrates as microspheres or particles is a ubiquitous issue in many biotechnology assemblies[1] including chromatography separation,[2] enzyme immobilization and catalysis,[3] drug release,[4] sensors[5] and even tissue engineering.[6] Success design of these assemblies relies on extensive understanding and accurate mapping the fundamental interaction laws of protein on surface. For this reason, there is a growing appreciation on exploring the relativity between the surface property of substrate and protein structural change. In particular, the surface curvature of substrate was generally discovered to play delicate role. The surface curvature, governed by the bulk size of substrate, would modulate many protein's adsorption characteristics including secondary and tertiary structure, thermodynamic stability and activity to protein-substrates size dependent pattern.[7-15] However, all of these substrates focus on convex surface of nonporous materials such as silica nanoparticles or carbon nanotubes.[7-17] For concave surface inner pores of porous microspheres, with curvature opposite to particles surface, the roles of pore curvature that governing protein behaviours is not well established.

Although the specific studies on pore curvature from micro-scale are scarce, macroscopic applications of porous microspheres have recognized the pore size as an essential property of substrates to tailor the proteins activity. For example, in enzyme immobilization, an obvious sensibility of protein to support pore size was found that hydrophobic macroporous resins could preserved more enzyme activity for lipase than mesoporous resins.[18, 19] Also in chromatography, pancreatic trypsin inhibitor was found unfolded fewer in large pore than narrow pores when its radius comparable to protein.[20] Further, some newly emerging superporous microspheres (mostly pore size > 100 nm) presented an excellent enhancement of protein recovery than traditional supports (pore size< 50 nm) during purifications of myoglobin, transferrin, bovine serum albumin, PEG-recombinant human granulocyte colony-stimulating factor, intact proteins solubilised by detergents.[21, 22] Except for many perspectives of the diffusion rate contribution to protein activity enhancement, the specific disturbance of pores curvature tailored by pore size is still unknown, which required more in-depth observation of protein molecules in confined pore space.

Microscopic observation of bound protein has been realized by current technology ensemble of circular dichroism (CD),[7, 8, 14, 15] infrared spectroscopy (IR),[9] atomic force microscopy (AFM), [23] dual polarisation interferometry (DPI),[24] surface plasmon resonance (SPR),[25] neutron reflection.[26] However, their

observation were limited on surface of flat chips or particles. Acquirement of sufficient protein details in pores chamber is still technically difficult. Furthermore, they only mapped the apparent molecular information such as aggregation, thickness, density and conformation enthalpy, but little account of the sub-molecular resolution details such as binding sites or specific unfolding domain.

The objective of this research was therefore to provide a first study examining how the pore curvature perturbed the protein structure, from macroscopic to microscopic by approaches including chromatography evaluation, confocal scanning, protein NMR hydrogen and deuterium (H/D) exchange experiments, molecular docking simulations. Among them, chromatography helped to reveal the interactive and unfolding behaviour of protein with pores wall of different curvature by examining their isocratic elution retention parameters. Confocal scanning was employed to supply the diffusion behaviours of protein in porous particles. NMR H/D experiments helped to open out residue-resolution information of proteins adsorption in pores such as unfolding degree, binding sites. Docking simulations of Autodock package based on binding energy ranking, the involved energy analyses was employed to confirm the detected preferred interaction zone by NMR methodology. Lysozyme was chosen as model protein in consideration of its extremely well-characterized structure and thoroughly documented data. Polystyrene microspheres of different average pores size range were selected as model substrate here, considering that their surface chemistries were identical with uniform density of phenyl and scarcity of other desirable homogeneraous porous microspheres with pores in nanometer range for protein size scale.

2 Materials and Methods

2.1 materials

Model protein, hen egg white lysozyme, was obtained from Sigma (cat. No. L-268). The solvents of deuterium oxide, deuterated hydrochloric acid and deuterated sodium hydroxide were all purchased from Sigma-Aldrich. HPLC grade acetonitrile (ACN) were obtained from Fisher Scientific. Polystyrene microspheres respectively with average pore size of 14nm, 30nm and 120nm were self-prepared by membrane emulsification and suspension polymerization according to our previous developed techniques.[27, 28] The average diameters of microspehers were determined by BET nitrogen adsorption/desorption and Mercury intrusion porosimetry measurements according to their applicable scope as shown in supporting materials.

2.1 Isocratic chromatography

Polystyrene microspheres with three pore sizes were respectively packed into chromatography columns. The adsorption and diffusion of protein in pores of columns were evaluated by two retention factors at isocratic chromatography with reverse phase chromatography mode considering the strong hydrophobicity of pendant phenyl group on polystyrene microspheres. Specifically, the adsorption retention factor (k'_{ad}) was measured by the ratio of protein's retention time at column in 5% acetonitrile mobile phase and its hold-up time in 100% acetonitrile mobile phase. The diffusion retention factor (k'_{di}.) was measured by the ratio of un-retained protein's retention time in 100% acetonitrile mobile phase and the acetone hold-up time at 100% acetonitrile mobile phase. Their retention times were measured using an SHIMADZU LC-20A chromatography system.

2.3 Laser scanning confocal microscopy imaging of protein diffusion in porous microspheres

Laser scanning confocal microscopy imaging was used to visualize protein diffusion in porous microspheres. Lysozyme was first labelled by FITC according to method from Teske et al.[29] Then the labelled lysozyme was incubated as probe proteins with microspheres of specific pore sizes for 2 hours. This incubation suspension was centrifuged in 10 kDa ultrafiltration filter to remove the unabsorbed FITC-protein, and obtain the suspension of microspheres adsorbed with protein. This suspension was finally observed with a Laser scanning confocal microscopy (TCS SP2 CLSM, Leica, Germany) at excited wavelength of 488 nm. The fluorescent images were acquired at 520–550 nm wavelengths.

2.4 H/D Exchange of adsorbed protein

The H/D exchange of lysozyme in microspheres of different pores follows procedures in Figure 1. Both lysozyme and the microspheres fully wetting beforehand were incubated in PBS buffer (pH=7.0) on rotary platform at 25℃ for 2 hours. The microspheres adsorbed with LYSOZYME molecules were packed into a column, according to our previously developed procedures.[30] Then the H/D exchange on microspheres was initiated by loading the label buffer (D_2O, PBS, pH*=6.8) into the microspheres packing column. After the given time, this H/D exchange reaction was quenched by loading quench buffer (D_2O, NaAC, pH* = 3.8) into above packing column, for such specific acid environment could inhibit exchange rate of backbone amide hydrogen on proteins to minimum. Finally, the labelled absorbed protein on microspheres was eluted by elution buffer (D_2O, acetonitrile, NaAC, pH* = 3.8) in exchange inhibition condition, then desalted by 3-kDa ultrafiltration filter and concentrated by lyophilizing at -70℃ before NMR detection. The unabsorbed control sample of free protein was prepared with same steps as above except for addition of microspheres.

2.5 NMR spectroscopy and sample preparation

All NMR experiments were recorded at 25°C on a Bruker 600 MHz Avance III spectrometer using a 5-mm Triple inverse TCI cryo-probehead equipped with a z-gradient. The lyophilized protein sample was dissolved into D_2O at pH 3.8 with 4 mg/ml labelled Lysozyme. The 2D NMR spectra of total correlation spectroscopy (TOCSY) was acquired with the dipsi2gpph19 pulse sequence from the Bruker library, in which the size of fid was 2048 data points in t2 and 256 increments in t1, the number of dummy scans 16 and number of scans was 24.

2.6 Hydrogen exchange data analysis

The assignments of NH-C_αH cross peaks signals in TOCSY spectra to the amide proton on side-chain of each residue referred to the reported 1H assignments of lysozyme at Biological Magnetic Resonance Bank (BMRB 4562). In order to eliminate the divergence of concentration and signal magnification between samples, the intensity of each peak was normalized to the nonexchanging reference peak of aromatic residue (H4-H5 on

Trp108). The H/D exchange rate ($v_{H/D}$) was calculated by following average loss percentage of residues' intensity in a fixed time as ten minutes here, where I_0 is the residues' intensity at zero time during H/D exchange and I_t is the residues' intensity exchanged after t time.

$$v_{H/D} = \frac{I_0 - I_t}{I_0 \cdot t} \quad (1)$$

2.7 Autodock

Because the matrix of polystyrene microspheres was covered with the pendant phenyl group, docking simulations was performed with lysozyme and phenyl ligand by the Autodock package 4.0 (Olson Laboratory, USA). The structure of lysozyme was retrieved from the PDB bank (1E8L). Phenyl ligand was built and optimized via Chemdraw 3D and Accelrys discovery studio (Accelrys, Inc. San Diego, USA). The protein's surface was divided into 6 grids with grid sizes of 60×60×60 and grid spacing 0.375 Å. The docking was conducted with the Lamarckian genetic algorithm and 20 docked conformations for each simulation to search for the minimum binding free energy of the protein–ligand complex. The binding free energy of an adopted protein–ligand confirmation was predicted, including the van der Waals, hydrogen bonding, electrostatics, desolvation, and torsional free energies. The possible conformations and binding zone were finally determined by visualization, energetic and cluster analysis.

3 Results and Discussion

3.1 Pore size effect on protein adsorption by chromatography

Chromatographic retention of biomolecule is a process limited by biomolecule affinity and diffusion with pores of stationary phase in column, and thus it becomes a comprehensive reflection of protein interaction, unfolding and transport behaviour in stationary phase.[31-34] Here, the chromatographic retention were specifically estimated by two derivations of general retention factor, i.e. the adsorption retention factor k'_{ad} and the diffusion retention factor k'_{di}. They were respectively related to the affinity of protein with pore wall, and the protein's accessible distribution in microsphere porous structure. They were designed aiming to normalize the divergence between columns such as the column's tube geometry and the supports packed density.

According to the definition of general retention factor that the sample residence time in stationary phase relative to its residence time in mobile phase during elution,[35] k'_{ad} was estimated by the ratio of protein's retention time in adsorbed state(t_R) to it in un-adsorbed state (t_u) at loading condition of 100% acetonitrile mobile phase. Consequently, k'_{ad} expressed how seriously a protein was retarded by binding strength of microspheres. It normalized the diffusion contributions from the diverse porous structure for protein transport through packing microspheres, and made the binding strength of microspheres comparable between different columns.

$$k'_{ad} = \frac{t_R - t_u}{t_u} \quad (2)$$

Beside of binding strength, k'_{ad} also reflect the degree of protein conformational change and structural unfolding. According to Brian's assumption,[36] when protein conformational change on hydrophobic surface follows first-order kinetics, the retention time of protein (t_R) was expressed by following factors as shown Eq.2, where L is the chromatographic column length, u is the flow rate, ε is intraparticle porosities, ε_p is interstitial porosities, K is the size exclusion distribution coefficient, α is adsorption equilibrium constant, ξ is the conformational change equilibrium constant. Further, t_u was expressed as no consideration of both terms of α and ξ because neither the adsorption nor the conformational change contributed for protein retention at this case. Then k'_{ad} can be simplified as a function of the conformational change equilibrium constant ξ as shown in Eq.3.

$$t_R = \frac{L}{u}\left[1 + \frac{1-\varepsilon}{\varepsilon K}\left(\varepsilon_p + \frac{1}{\alpha} + \frac{1}{\alpha\xi}\right)\right] \quad (3)$$

$$k'_{ad} = \frac{t_R - t_u}{t_u} = \frac{1}{\alpha} + \frac{1}{\alpha\xi} \quad (4)$$

$$t_u = \frac{L}{u}\left[1 + \frac{1-\varepsilon}{\varepsilon K}\left(\varepsilon_p\right)\right] \quad (5)$$

According to above, the macroscope effect of pore size on protein's adsorption and unfolding was assessed by evaluating k'_{ad} of lysozyme, at a range of columns packed with polystyrene microspheres with significant differences in pore diameter from 14 nm to 120 nm at reversed phase chromatographic mode. As illustrated in Fig.2, k'_{ad} has a first sharp decrease at mesopores range from 14 nm to 30 nm, indicating that lysozyme resides shorter in large porous channel than small ones. The binding strenth of lysozyme with pores wall was thus inspected to be significantly weakened and its unfolding was also alleviated with pore size enlargement at this pore range. Comparatively, extended to macroporous range from 30 nm to 120 nm, k_{ad}' become steady with only slight rise. It demonstarted that lyszoyme adsorption was not sensible to large pores geometry and apparent sensibility only existed in mesoporous range. At this range, the size of lysozyme[37] (3.0 nm × 3.0 nm × 4.5 nm) was just comparable to microspheres pore size (14nm to 30nm) with their ratio about 3 to 10. This comparable ratio interestingly accorded with the previously observations on protein structural change with pore size in porous microspheres, such as the fewer unfolding trend of pancreatic trypsin inhibitor (2.0 × 3.0nm) adsorbed on C18 chromatography media from 10 to 12 nm pores, and the activity enhancement of lipase (6.92 × 5.05 × 8.67) immobilized on carriers from 20 to 120nm. Such size effect was also supported by reportorial views on simulations of protein behaviours by molecule dynamics calculating polymers structure change in confined space.[38] During their evaluating the interaction free energy and entropy of polymer in nano-slits, molecule tend to keep more compact structure in wider space and experienced a drastic structural change in narrow space, which is comparable to

the polymer size dimension. Therefore, summary of all above protein adsorption events demonstrated that there must be a critical scope for pore geometry to take effect on protein structural change, during which wider pores would facilitate better preservation of protein structure.

From another point, the diffusion retention factor, k'_{di} specifically assessed the distributions of pores accessible to protein in microspheres due to size exclusion effects. It estimated the retention time ratio of two molecules including protein and acetone both at loading condition of 100% acetonitrile mobile phase when none adsorption was involved. Interestingly, contrary to k_{ad}' for adsorption, k'_{di} present a reverse upward tendency as a continuously prolonging lysozyme residence with pores enlarging. It might be attributed to the lysozyme's different accessibility in these microspheres matrix, which was visualized by confocal microscopy as that lysozyme enriched at outside layers in both microspheres with pores diameter 30nm and 14nm, whereas diffuse deep into inner core in microspheres with pores diameter 120nm (Fig.3). It indicated that comparatively, macroporous microspheres provide more inner mass transfer space for lysozyme and thus prolonged its retention at this diffusion controlled chromatographic mode.

3.2 Protein unfolding pattern in porous channel by NMR

Since protein's retention in different pores was highly related to protein's unfolding, we further directed our insight into microscopic and in situ description of the protein unfolding degree on adsorbents by H/D exchange and NMR protocol of TOCSY spectrum (Figure 4). The intensity of each TOCSY crosspeaks for residue's amide proton was normalized to avoid diversities between concentration and detections (Fig. 4 b). Their signal decay reflects the residue exposure extent and corresponding local structural change of protein. From the overall look, lysozyme adsorbed in all porous microspheres presented a significantly diminishment of residues signals intensity compare to its natural state. Specifically, the disorder structures including coil, bend and turn fragments (residues from 65 to 80, 110 to 119), were less protected and lost more signal intensity than the secondary structure domains (residues from helix1, helix2, sheet1, helix3 and helix4), because of their more flexibility to exposure and exchange. This selective exchanging pattern of proton signals resembled our previous rules at phenyl-Sepharose microspheres. However, comparatively, at polystyrene microspheres, lysozyme underwent more significant loss of signal intensity at secondary structure, which reflected that protein denatured much seriously and couldn't sustain the molten global state as it on weaker hydrophobic phenyl-sepharose.

Furthermore, the influence of pore size on the exposure of lyzoyme was far more pronounced than chromatography retention analysis. Lysozyme in 14nm and 30nm pores showed marked intensity loss for most signals than its free state, suggesting their structures were disrupted and unfolded seriously. When pore size rises to 120 nm, the proton intensity of most residues had a sharp rise, reflecting that most structures and more compactness of protein molecule were preserved against exchange than in small pores. For specific distinct fragments, the protection degrees of these states also varied. We found some structure lost more intensity when pores enlarged such as the random sequence of bend, turn and coil structures around residue 20, indicating the residue at disorder domain had greater sensibility to protein molecule's unfolding perturbation.

3.3 Protein contact sites in porous channel

Here the binding of the residues on pores wall was dominated by hydrophobic interaction arise from the dense phenyl group on pores polystyrene wall. Therefore, only the hydrophobic residues exposed on protein surface have priority to be recognized by adsorbed surface, as demonstration in their significant contributions for binding, retention and selectivity in protein chromatography.[14-16, 30] Beside this, another feature of binding sites is their slower exchange dynamics rate than un-adsorbed protein, because interface adsorption also has a local effect to protect binding residues against H/D exchnage.[39] Therefore, aiming to identify the specific residues with above characteristics, we first picked out the hydrophobic residues (Phe, Met, Leu, Cys, Tys, Val, Tyr, Ala, His) of protein by their Miyazawa's hydrophobia scales (Fig. 5, colour labelled dotted).[40] Then, the protected residues with slow H/D exchange rate ($\nu_{H/D}$) were determined by recognizing the H/D exchange rate ratio (θ) of adsorbed and un-adsorbed samples below zero (Fig. 5, red shadow).

$$\theta = \frac{\nu_{H/D(unadsob)} - \nu_{H/D(adsob)}}{\nu_{H/D(unadsob)}} \times 100\% \quad (6)$$

Finally from them, we picked out the exposed sites as possible binding sites (Figure 6, residue name labelled) by their solvent accessible surface area (SASA >10%), which was calculated by MOLMOL program with a typical probe radius of water 1.4 Å and lysozyme structural data (from Protein Data Bank code: 1E8L).

Figure 5 showed that except a few protected binding residues, most hydrophobic residues of lysozyme presented a makeable loss of intensity with θ high above zero. It indicated that even the inner core of lyzoyme global molecules experienced great disruption because of such strong hydrophobic interaction induced adsorption. The possible binding sites of protein were respectively mapped to 6 residues (Val2, Phe3, Ala11, Ala107, ALA 122 and CYS 127) for microspheres of 14 nm pores, 4 residues (Phe3, Ala122, Cys127, Leu 129) for 30 nm pores, and 2 residues (Trp123, Cry 127) for 120 nm pores. They presented a decrease tendency with pore size increased. It demonstrated that fewer hydrophobic sites were exposed to attain phenyl on pores walls, and consequently the contact area of lysozyme with pores wall might gradually shrink with the pores size enlarged.

Above NMR detected binding sites were further evaluated from another point of view with binding free energy shown in Fig.6. Three possible interaction zones of lysozyme to phenyl ligand were first searched out by ranking the binding energy utilizing Autodock package and coarse-grained simulations (Fig.6 left column). All of these zones apparently tend to anchor the phenyl ligand at middle of lysozyme rich in hydrophobic residues (Fig.6 red lines in left column), and far away from hydrophilic residues zones (Fig.6, green lines in left column). It was inferred that the reorganization of lyszoyme to phenyl most likely depend on the densely distributed area of many hydrophobic residues but not the separated residues with high hydrophobicity scale. Then,

the anchoring zones by dock were continuously magnified into residues description (Fig.6 middle column) as the hydrophobic active sites (red labelled) and the adjacent hydrophilic inert residues (black labelled). As a comparison, most binding sites by NMR (Fig.6 right column) can be respectively found in docking sites assembly (Fig.6 middle column). Such consistency between them indicated that the interface adsorption of lysozyme at pore wall was still essentially governed by binding energy.

Interestingly, if continue to attribute the NMR determined binding sites to docked zones with top three lowest binding energy (Fig.6 right column, A,B and C in brackets), lysozyme was observed to present a decreasing diversity of zones with pore size increasing, as that most zones (A, B and C) were adopted in pore channel of 14nm, but fewer (B and C) in 30nm and only one (C) in 120nm pores. Such tendency indicated that lysozyme molecule might be unfolded more greatly in narrower pores, where the hydrophobic interaction force tend to induce multiple protein adsorption conformations more significantly. Also the sever unfolding of lysozyme in narrow pores of 14 nm even make the zone A(Fig.6 left column, zone A) deep in active cleft possible (Fig.6 right column ALA 107), where the residues actrualy has greatest steric hindrance to contact with the fixed ligand on wall surface. Comparatively, lysozyme seemed to prefer to bind at zone B and C with larger binding energy but easier contacted position at cover of protein molecule.

3.4 Modelling the interaction of protein with pores innerface

To qualitative describe and elucidate the basis for above pore geometry effects, we directed our interest into the intrinsic mechanism of protein interacted area development tailored by different pores curvature. A simplified model (schematic illustration in figure 7 left) was proposed as follows equation, assuming that the protein molecule is a hard sphere (radius, r) and its interacted area with pore wall appeared as the spherical crown (radius, R). The limited possible interacted distance(h) between the curve surfaces of protein and pore was set to 3 Å according to the shortest distance calculated by Autodock between groups on lysozyme and phenyl ligand, and the protein size (r) selected the average radius of lysozyme as 2 nm.

$$S_{protein}[R,r] = \frac{\pi r(2Rh + h^2)}{R - r + h} \quad (7)$$

Thus, the interacted area of protein ($S_{protein}$) can be plotted as the function of pores diameter (R) in figure 7. It presented the development of $S_{protein}$ curve has two stages, i.e., the first sharp decline of $S_{protein}$ at micropores range (radius <15 nm), and the second low plateau of $S_{protein}$ at macropores range (radius 15 nm to 200 nm). It indicated that the dependence of $S_{protein}$ on pore size only existed in micro-pores range. Its quick decrease of $S_{protein}$ with pores just explained well the much shortened chromatographic retention of lysozyme at microspheres pores from radius 7 nm to 15 nm, and thus confirmed the aforementioned speculation that unfolding and binding strength of protein were determined by protein interacted area. At the second stage of macropores range (radius from 15 nm to 200 nm), the weak dependency of $S_{protein}$ on pores size just explained well the slight changes of lysozyme's retention and binding sites at macroporous microspheres (pore diameter from 30 nm to 120 nm).

Above hypothesis that the protein structure perturbation dependence on interacted area is a curvature effect may be further supported by previous studies on particles-protein conjugates from silica-nanoparticles to carbon nanotubes.[7-15] They also observed curvature effect on protein structural change by particles size. However, they presented a different direction just reverse to pores events, as that smaller particles lead to more activity and stability of protein. Such reverse trend may be attributed to their surface is convex with opposite curvature to concave of pores wall. In order to validate this speculation, we propose another model and extended the calculation of $S_{protein}$ to much wider size range (Figure 7, right). Interestingly, we found $S_{protein}$ curves of particle showed a mirroring tendency to that of pores, which make the $S_{protein}$ also developed two stages but with a ascendant direction. The dependence of protein structure on particles size represents as that the contact area rapid rise with particles size enlarging until to a critical size, and was flatten out after that. Such calculated tendency was also in consistent with the practical adsorption rules on particles. Comparing these two curvature models, we could find the pores always induced much more interacted area of protein than particle size model, implying that the protein in pores was perturbed greater by interacted solid surface, and might be bound more tightly and presented longer residence in elution.

4 Conclusions

This study, for the first time, from multiple scales quantitatively elucidated the pore curvature (size) effect on protein conformational change. Tendency in retention, binding sites and solvent exposure degree of bound lysozyme detected by NMR and chromatography corresponded well with the change of protein adsorption area induced by pore curvature according to model calculation. In particular, they showed that the binding affinity, unfolding extends, and binding sites of lysozyme adsorbed on porous polystyrene microspheres strongly depend on their pore size or curvature. A critical pore size was discovered to trigger such curvature effects. After this pore size and into macro pores range, the significant dependence would disappear. For another surface of opposite curvature for nanoparticle, the rule was similar but with the opposite direction. Another should be noted that all these evaluations focus on the average behaviour of lysozyme molecules population. Aim to clarify the pore curvature and size effect, other individual events beyond average have to be ignored including other pores out of the average size in one microspheres, multiple protein structure in one adsorption, and oversimplified contact area modelling such as without considering solvent effect contribution.

With understanding how biomolecules adsorption was affected by the topology of pore surface, the desirable control of their biology function can be achieved. This may give rise to purposely design of novel porous materials in chromatography, enzyme carrier, biosensors or drug delivery carrier, and also assist to discriminate the target protein to match above pore geometry.

Acknowledgment

Thanks for the supports from National Natural Science Foundation of China, programs (No. 21336010), (No. 21106161) and (No. 20820102036). Another thank for discussions with Prof. Martin Lundqvist about protein contact area calculations.

Note and references

[a] *National Key Lab of Biochemical Engineering, Institute of Process Engineering, Chinese Academy of Sciences, Zhong Guan Cun Bei Er Tiao #1, Beijing, 100190, China*

[5] ** ghma@home.ipe.ac.cn, zgsu@home.ipe.ac.cn; Fax/Tel:+ 86-10-8262-7072*

[b] *Chemical Engineering School, Hebei University of Technology,Guang Rong Dao, Tianjin, 300130,China*

1 J.B. Fan, C.Huang, L. Jiang, S.T. Wang, Journal of Materials Chemistry B, 2013, 1, 2222;
2 C.S. To Brian, M. L. Abraham, Journal of Chromatography A, 2007, 1141, 191;
3 P.Wang, S D.Waezsada, A. Y. Tsao, B. H. Davison, Biotechnology and Bioengineering, 2001, 74, 249;
4 L.S. Liu, S.Q. Liu, S.Y. Ng, M. Froix, T. Ohno, J. Heller, Journal of Control Release, 1997, 43;
5 C. L. Baird, D. G.Myszka, Journal of Molecular Recognition, 2001 , 14, 261;
6 H.J. Chung, T.G. Park, Tissue Engineering Part A, 2009, 15, 1391;
7 M. Lundqvist, I. Sethson, B. H. Jonsson, Langmuir, 2004, 20, 10639;
8 A. A. Vertegel, R. W. Siegel, J. S. Dordick, Langmuir, 2004, 20, 6800;
9 P. Roach, D. Farrar, C. C. Perry, Journal of the American Chemical Society, 2006, 128, 3939;
10 L. Fei, S. Perrett, International Journal of Molecular Sciences, 2009, 10, 646;
11 Z.C. Wu, B. Zhang, B. Yan, International Journal of Molecule Sciences, 2009, 10, 4198;
12 P. Asuri, S. S. Karajanagi, H. Yang, T. J. Yim, R. S. Kane, J. S. Dordick, Langmuir, 2006, 22, 5833;
13 C.J. Wang, U. B. Jensen, G. V. Jensen, S. Shipovskov, V. S. Balakrishnan, D. Otzen, P. J. Skov, F. Besenbacher, D. S. Sutherland, Nano Letters, 2011, 11, 4985;
14 W. Shang, J. H. Nuffer, J. S. Dordick, R. W. Siegel, *Nano Letters*, 2007, **7**, 1991;
15 W. Shang, J. H. Nuffer, V. A. Mun˜iz-Papandrea, W. Colo´n, R. W. Siegel, J. S. Dordick, *small*, 2009, **5**, 470;
16 P. Asuri, S. S. Karajanagi, H. C. Yang, T. J. Yim, R. S. Kane, J. S. Dordick, *Langmuir* 2006, **22**, 5833;
17 S. S. Karajanagi, A.A. Vertegel, R. S. Kane, J. S. Dordick, *Langmuir* 2004, **20**, 11594;
18 Y. Li, F. Gao, W. Wei, J.B. Qu, G. H. Ma, W.Q. Zhou, *Journal of Molecule Catalysis B: Enzymatic*, 2010, **66**,182-189
19 J. A. Laszloa, M. Jacksona, R. M. Blancob, *Journal of Molecule Catalysis B: Enzymatic*, 2011, **69**, 60–65
20 J. L. M. McNay, E. J. Fernandez, *Biotechnology & Bioengineering*, 2001, **76**, 224;
21 Y. Q. Zhai, W. Q. Zhou, W. Wei, J. B. Qu, J. D. Lei, Z. G. Su, G. H. Ma, *Analytica Chimica Acta*, 2012, **712**, 152;.
22 J. B. Qu, Z. G. Su, G. H. Ma, *Journal of Chromatography A*, 2009, **1216**, 6511;
23 D. T. Kim, H.W. Blanch, C.J. Radke, *Langmuir*, 2002,18, 5841;
24 M. S. Lord, M. H. Stenzel, A. Simmons, B. K. Milthorpe, *Biomaterials*, 2006, **27**, 1341;
25 A.W. Sonesson, *Colloids and Surfaces B: Biointerfaces*, 2007, **54**, 236;
26 J. R. Lu, X.B. Zhao, M. Y seen, *Current Opinion in Colloid & Interface Science*, 2007, **12**, 9;
27 D.X. Hao, F.L. Gong, W. Wei, G.H. Hu, G.H. Ma, Z.G. Su, *Journal of Colloid and Interface*, 2008, **323**, 52;
28 W.Q. Zhou, T. Y. Gu, Z. G. Su, G. H. Ma, *Polymer*, 2007, **48**, 1981;
29 C.A. Teske, M. Schroeder, R. Simon, J. Hubbuch, *The Journal of Physical Chemistry B*, 2005, **28**, 13811;
30 D.X. Hao, C. Sandström, Y.D. Huang, L. Kenne, J.C. Janson, G.H. Ma, Z.G. Su, *Soft Matter*, 2012, **8**, 6248;
31 A. W. Purcell, M.I. Aguilar, M. T. W. Hearn, *Analytical Chemistry* 1999, **71**, 2440;
32 T. T. Jones, E. J. Fernandez, *Journal of Colloid and Interface Science,* 2003, **259**, 27;
33 R. I. Boysen, A. J.O. Jong, M.T.W. Hearn, *Journal of Chromatography A*, 2005, **1079**, 173;
34 M. Renata, M. Wojciech, P. Wojciech, D. A. Atkowski, *Journal of Chromatography A*, 2010, **1217**, 2812;
35 L.S.Ettre, Nomenclature For Chromatography, *Pure and Applied Chemistry*, 1993, **65**, 819;
36 B. C.S. To, A. M. Lenhoff, *Journal of Chromatography A*, 2008, **1205**, 46;
37 C. C. F. Blake, D. F. Koenig, G. A. Mair, A. C. T. North, D. C. Phillips, V. R. Sarma, *Nature*, 1965, **206**, 757;
38 Y. Ren, J. Gao, W. Ge, J.H. Li, G. H. Hu, *Chinese Science Bulletin*, 2008, **53**, 2599;
39 D. A. Keire, D.G. Gorenstein, *The Bulletin of Magnetic Resonance* 1992, **14**, 57;
40 M. E. Lienqueo, A. Mahn, J. A. Asenjo, *Journal of Chromatography A*, 2002, **978**, 71.

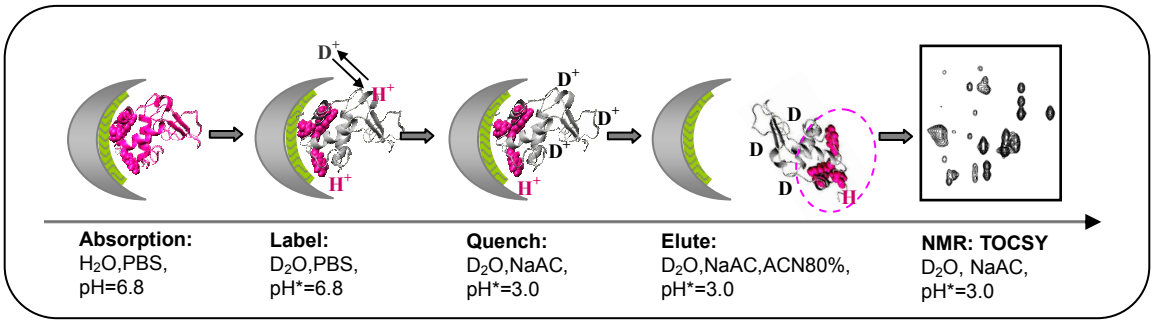

Figure 1 The H/D exchange and NMR procedures of lysozyme adsorbed in porous polystyrene microspheres

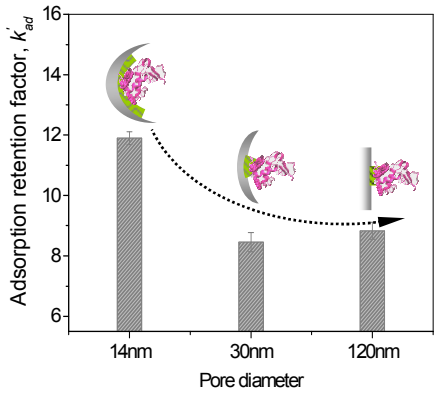

Figure 2. The adsorption retention factor of lysozyme adsorbed in polystyrene microspheres of different pore diameter.

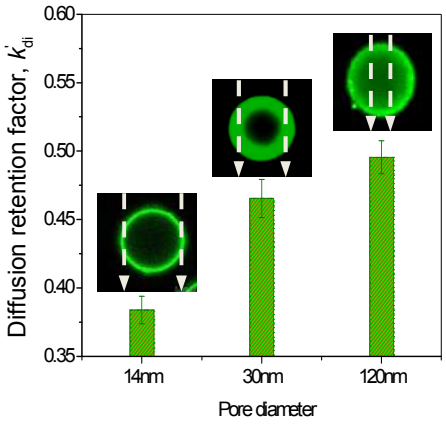

Figure 3. The diffusion retention factor and confocal image of lysozyme adsorbed in polystyrene microspheres of different pore diameter.

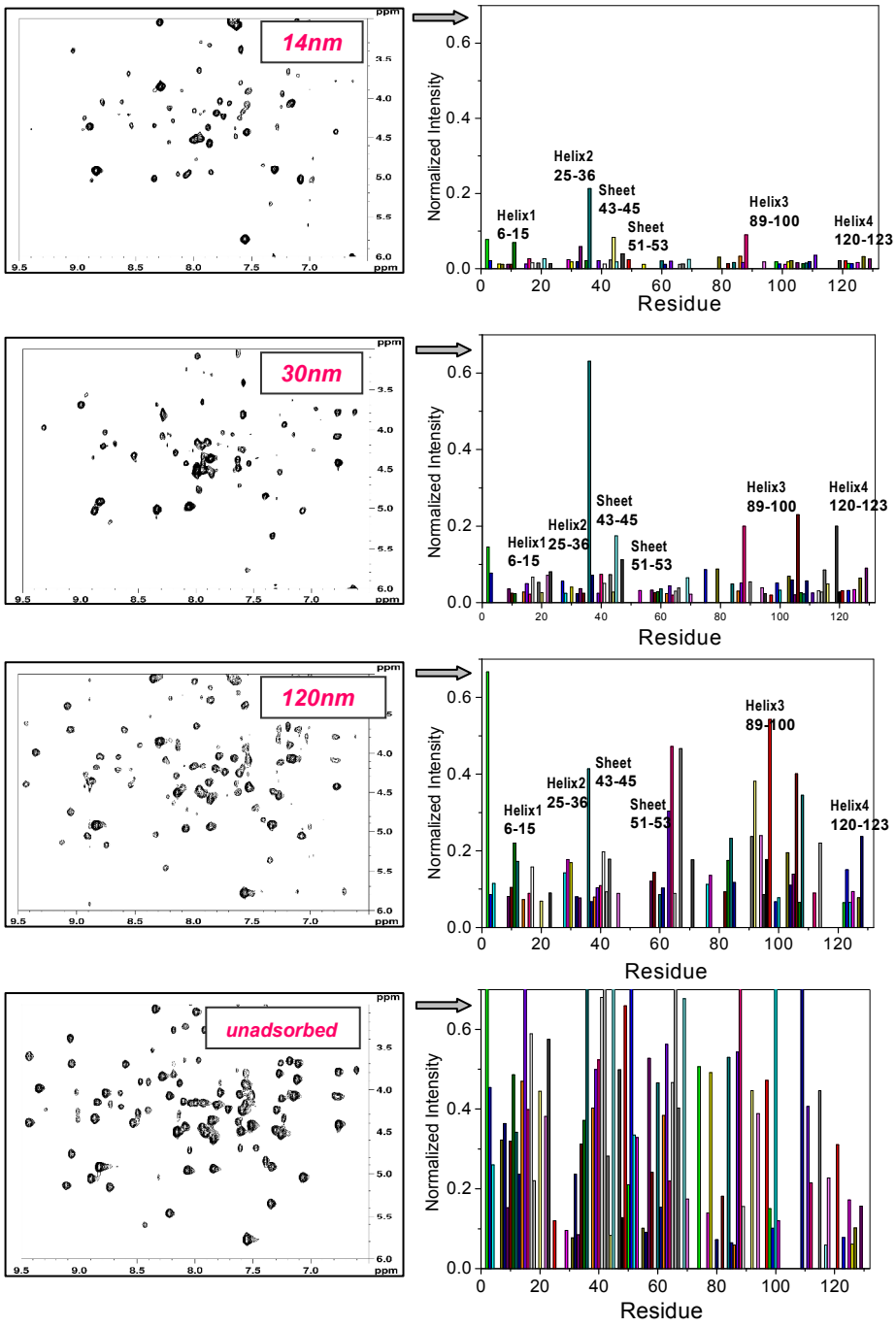

a. TOCSY spectrum b. Residue's nomorlized intensity

Figure 4. The TOCSY spectrum of lysozyme in polystyrene microspheres of different pore diameter. 1-5 random, 6-15 helix1, 16-24 random, 25-36 helix2, 37-42 random, 43-45 sheet, 46-50 random, 51-53 sheet, 54-88 random, 89-100 helix3, 101-119 random, 120-123 helix4, 124-129 random

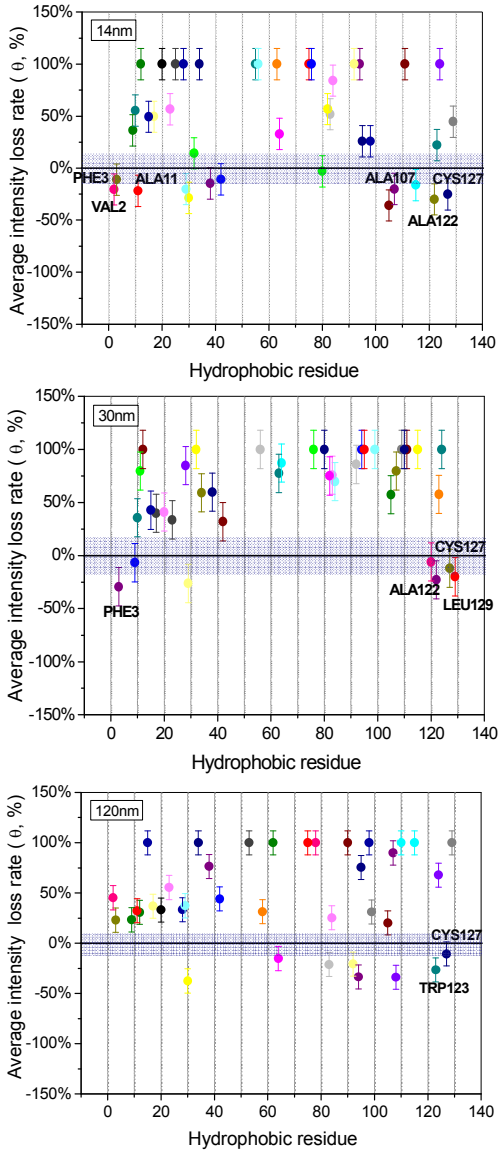

Figure 5. The intensity loss rate of all hydrophobic residues of lysozyme, and the possible binding sites (name labeled) in polystyrene microspheres of different pore diameter.

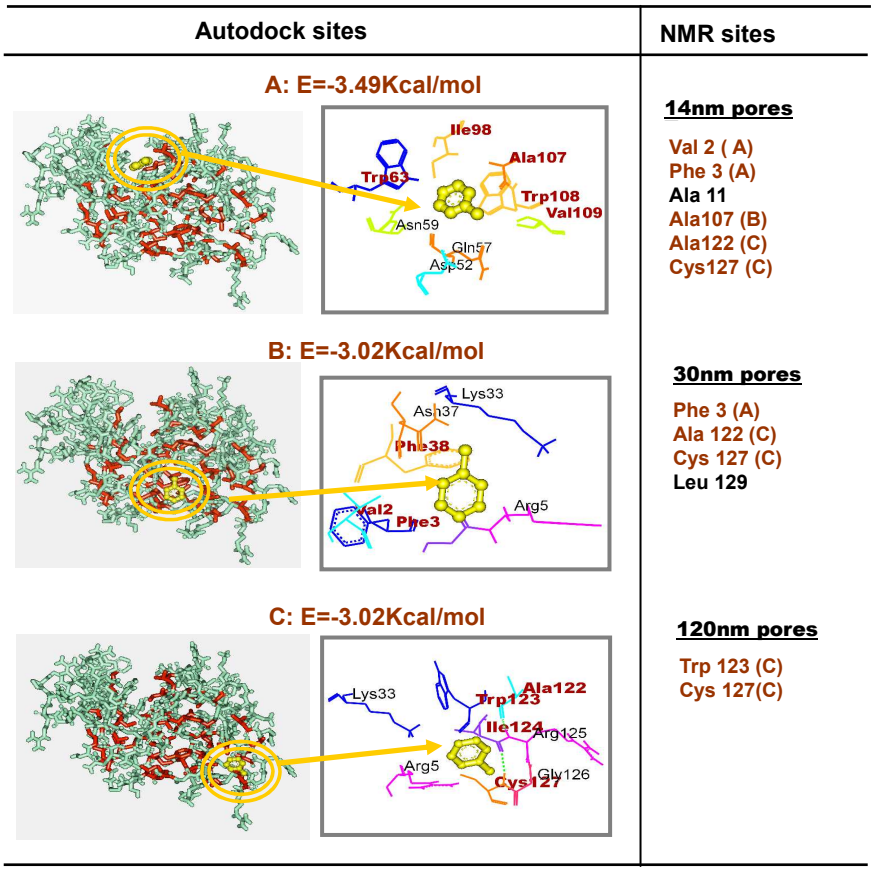

Figure 6. The ligand binding conformation and the interacted sites by Autodock, and the comparisons with NMR detected sites

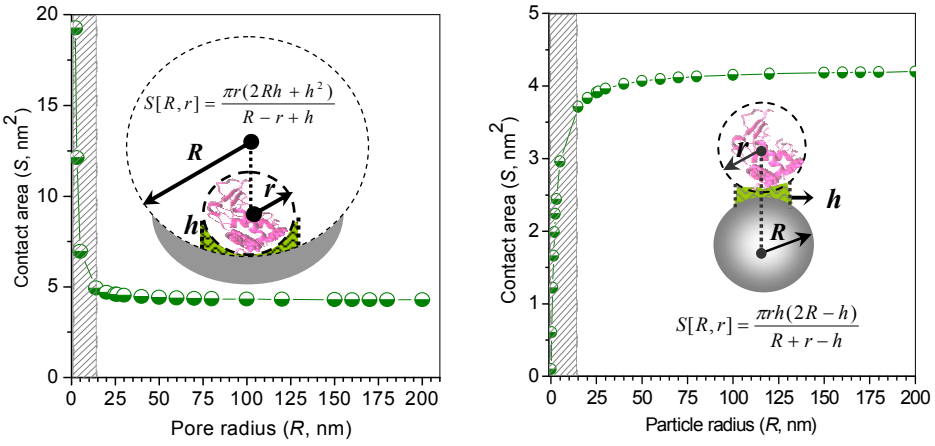

Figure 7. Contact surface area of lysozyme with pore radius (right) and particles radius (left). S, contact area; R, pore or particles radius; r, protein radius; h, hydrophobic interaction distance